JOURNAL OF MAGNETIC RESONANCE **135,** 373–379 (1998)
ARTICLE NO. MN981608

Surface and Gradiometer Coils near a Conducting Body: The Lift-off Effect

B. H. Suits,*[,1] A. N. Garroway,† and J. B. Miller†

*Physics Department, Michigan Technological University, Houghton, Michigan 49931; and
†Code 6122, Naval Research Laboratory, Washington, DC 20375-5342

Received July 6, 1998

The use of surface coils in magnetic resonance is widespread. Examples include MRI, detection of subsurface aquifers by NMR, and, more recently, landmine detection by nuclear quadrupole resonance. In many of these cases a finite-sized sample to be examined is contained within a larger medium that is a poor electrical conductor, and eddy currents induced by the RF fields provide a loss mechanism that reduces the effective quality factor Q of the transmitter and receiver coils. Here the losses induced in a circular surface coil (a horizontal loop antenna) separated a distance from a dissipative medium are calculated and compared to measurements. It is shown that often the overall efficiency of the coil for magnetic resonance can be improved by displacing the coil away from the conducting medium a prescribed "lift-off" distance. The use of a gradiometer as a surface coil is also examined, and it is shown by theory and experiment that in certain circumstances such a gradiometer can be more efficient than a conventional surface coil for inspection of conducting media.

Key Words: **magnetic resonance; NMR; NQR; MRI; surface coils; sensitivity; signal-to-noise ratio; lift-off; gradiometer; small loop antenna; dissipative media.**

INTRODUCTION

Magnetic resonance signals are typically weak and must compete with undesirable signals from thermal noise. Moreover, substantial RF power is required for the transmitter, especially when specimens are large. It is well known that the use of a high-Q receiver coil and/or transmitter coil is advantageous, since the signal-to-noise ratio (SNR) scales as $Q^{1/2}$ and, similarly, the required RF power to create a given magnetic field strength scales as $1/Q$. Any dissipation in the coil (receiver or transmitter) reduces Q. The usual loss mechanism is the resistive loss in the coil, but sample losses in a nearby conducting medium also reduce Q, leading to a decrease in SNR and an increase in the required transmitter power. Examples include patient loss in MRI (*1, 2*) and RF loss in wet soils (*3*) as seen for NMR study of subsurface aquifers (*4*) and for landmine detection by nuclear quadrupole resonance (*5–8*). The work here is primarily motivated by a need to optimize SNR for landmine detection, though the results can be expected to be applicable in general.

In many cases, obtaining signals from only a small region within the conducting medium is desired (MRI) or is practical (aquifers and landmines). In that case, surface coils are useful to "focus" the RF energy and signal pickup sensitivity to a smaller region of interest. At the same time the more focused RF field results in less dissipation in the surrounding medium and thus a better SNR (*1, 9*).

The loss mechanism can be easily understood. The RF magnetic field B_1 of frequency ω created in a coil induces eddy currents in nearby conducting media. We specialize to the case of a "poor conductor" for which the RF skin depth is large compared to coil dimensions and, correspondingly, the magnetic fields created by these eddy currents can be neglected in comparison to the field B_1. However, these eddy currents induce an ohmic loss in the medium. It has also been suggested that significant dielectric losses due to the presence of RF electric fields may also be present when the coil is close to the medium (*9*). Satisfactory results were obtained here without consideration of such dielectric losses.

An improvement of SNR with a small lift-off is known qualitatively (*2*) in the MRI community. Below we derive explicit expressions for the electrical dissipation and an effective measure of the SNR for measurements of a small sample in a conducting medium using a simple, circular surface coil that is displaced a distance h along its axis ("lift-off") from the medium and compare with experimental data. This is a generalization of the ($h = 0$) calculations of Harpen (*10*) and those of Wang *et al.* (*11*). We find that a lift-off of a fraction of a coil radius can improve the overall SNR and, of course, reduces the power deposition and total required transmitter power.

For a circular surface coil, which produces a dipole field at large distances, the RF field falls off fairly rapidly so that, in practice, sample regions approximately one coil radius deep and one coil diameter across can be observed. Following Harpen's analysis (*10*) it is straightforward to show that 83% of the power loss occurs outside one coil radius and 42% occurs outside two coil radii. That is, most of the power loss occurs at

[1] To whom correspondence should be addressed. Physics Department, Michigan Technological University, 1400 Townsend Dr., Houghton, MI 49931-1295. E-mail: suits@mtu.edu.

1090-7807/98 $25.00

distances where the RF field is too small to be effectively used for magnetic resonance. Hence, it therefore would be useful to employ a coil whose field falls off even more rapidly at large distances. Accordingly, theory and measurements were also pursued for the use of an axial gradiometer surface coil, comprising two circular surface coils displaced a distance b along their common axis and arranged so that the circulating currents oppose one another. At large distances, such a coil produces a magnetic quadrupole field. As we will show below, the dissipation for such a coil occurs almost entirely within a depth of one coil radius and the resulting *SNR* may be improved compared to the simple circular coil.

The general theory for the simple circular coil and the gradiometer coil near the surface of an infinite conducting medium is presented in the next section, along with corrections for finite media. This is followed by a comparison with measurements made in the laboratory.

THEORY

We start by computing the extra losses for a simple circular NMR coil made from thin wire in the vicinity of a semi-infinite poorly conducting medium and then apply corrections for a finite-sized medium. By poorly conducting what is meant is that the magnetic field due to currents induced in the medium can be neglected and that the skin depth is large compared to the size of the coil. We neglect capacitive effects between the coil and the medium, which will give rise to additional loss when the coil is very near the medium. The calculations below are a generalization of previous calculations performed for a circular loop surface coil of radius a resting in the x–y plane at $z = 0$, on the surface of a conducting medium occupying the half space $z < 0$ (*10*).

The time-averaged electrical power, P, lost in a poorly conducting medium in the presence of an RF magnetic field with angular frequency, ω, and amplitude, $\mathbf{B}_1$, which has a corresponding vector potential, **A,** in the Coulomb gauge, is given in the long wavelength limit by (*10*)

$$P = \frac{1}{2}\,\sigma\omega^2 \int_{\text{vol.}} \mathbf{A}\cdot\mathbf{A}\; d\tau, \qquad [1]$$

where σ is the conductivity of the medium and the integral is over the volume of the medium. For a circular loop of radius, a, with its axis along z and in the plane $z = 0$, **A** is given in cylindrical coordinates by the Lipschitz–Hankel integral (*12, 13*)

$$\mathbf{A} = \frac{1}{2}\,\mu_0 I a \mathbf{a}_\theta \int_0^\infty e^{-k|z|} J_1(kr) J_1(ka)\, dk, \qquad [2]$$

where I is the current in the coil, μ_0 is the permitivity of free space, and $\mathbf{a}_\theta$ is the azimuthal unit vector. Note that $\nabla\cdot\mathbf{A} = 0$. After some manipulation, we find that the losses in a poorly conducting half-volume extending from $z = h$ ($h > 0$) to $z = \infty$ are

$$P_\infty(h) = \frac{\pi}{8}\,\mu_0^2\,\sigma\,\omega^2\,I^2\,a^3\,f\left(2\frac{h}{a}\right) \equiv \frac{1}{2}\,I^2\,r_L(h), \qquad [3]$$

which defines the effective series resistance, r_L, due to losses in the medium. The function, f, is

$$\begin{aligned} f(\beta) &\equiv \int_0^\infty d\kappa \left[\frac{J_1(\kappa)}{\kappa}\right]^2 e^{-\kappa\beta} \\ &= \frac{1}{2\pi}\int_0^\pi [\sqrt{\beta^2 + 2 - 2\cos\phi} - \beta](1 + \cos\phi)\, d\phi \\ &\approx \left[\frac{8}{3\pi^2}\tan^{-1}\left(\frac{\pi}{4\beta}\right)\right]. \end{aligned} \qquad [4]$$

The second form of the integral in eq. [4] is due to Watson (*13*). Either of the two integral forms can be treated numerically, though the elliptic form converges much more rapidly and is preferred. From examination of results of numerical integration and series expansions for large and small h/a, we have discovered that the approximate form shown in eq. [4] is adequate for many practical calculations. The function $f(\beta)$ obtained using numerical integration and the approximation are compared in Fig. 1a. Note that $f(0) = 4/3\pi$ and that eq. [3] agrees with previous calculations (*9, 10*) for $h = 0$.

The losses for a conducting medium of infinite width but with a finite depth, D, are then given by

$$P_D(h) = \frac{\pi}{8}\,\mu_0^2\sigma\omega^2 I^2 a^3\left[f\left(2\,\frac{h}{a}\right) - f\left(2\,\frac{h+D}{a}\right)\right]. \qquad [5]$$

We have been unable to find a simple form for the case of a conducting medium with a finite width. However, an approximate result can be computed for the case where the width is large compared to the coil radius. In that case, the asymptotic form for **A** can be used (*12*). The losses from a region of infinite depth but restricted to the region $r > R$, with $R \gg a$, are

$$P_{r>R}(h) \approx \frac{\pi}{8}\,\mu_0^2\sigma\omega^2 I^2 a^3 \times \frac{1}{16}\left[\frac{3a}{R}\tan^{-1}(R/h) - \frac{ha}{R^2 + h^2}\right], \qquad [6]$$

and thus the losses within the region $r < R$ are given by the quantity $[P_\infty(h) - P_{r>R}(h)]$.

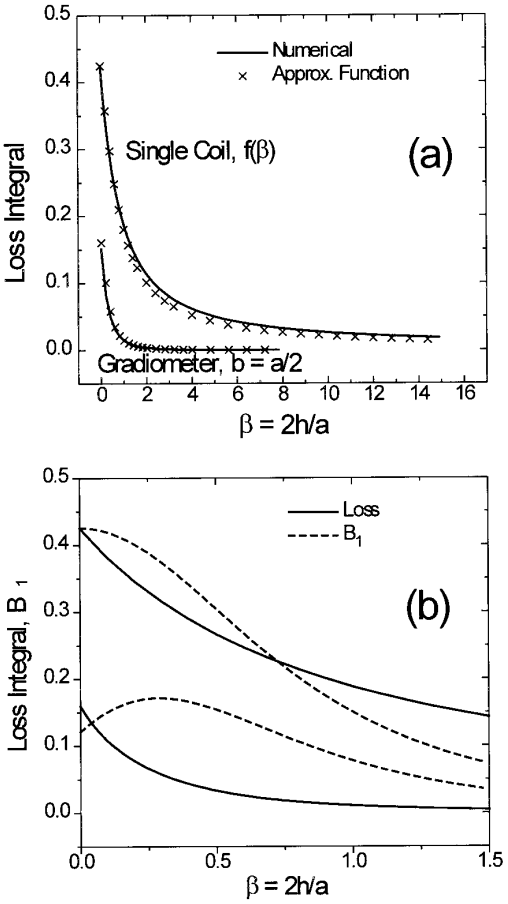

FIG. 1. (a) The loss integral for the single circular coil (Eq. [4]) and the gradiometer coil with $b = a/2$ (from Eq. [10]) computed numerically (solid line) compared to calculations using the approximate functional form (crosses) from Eq. [4]. (b) A comparison of the functional dependence of the loss integrals (solid lines) from (a) and the magnitude of the corresponding RF $\mathbf{B}_1$ fields (dotted lines) at $z = 0$ for small values of h. The magnitude of the $\mathbf{B}_1$'s have been scaled so that the value for the circular coil matches the loss integral at $h = 0$.

The magnetic field along the axis of the coil is given by the well-known expression

$$\mathbf{B}_1(z) = \frac{\mu_0}{4\pi} \frac{2\pi a^2 I}{(a^2 + z^2)^{3/2}} \mathbf{a}_z. \qquad [7]$$

The signal-to-noise ratio, *SNR*, for a tuned and matched coil will depend on the square root of the quality factor of the coil, Q, and the size of the induced EMF from a distant sample. For a coil inductance, L, with a series resistance, r_0,

$$\frac{1}{Q} = \frac{r_0}{\omega L} + \frac{r_L(h)}{\omega L} = \frac{1}{Q_{\text{inf}}} + \frac{1}{Q_L}, \qquad [8]$$

where Q_{inf} is the quality factor in the absence of the poorly conducting medium. The size of the induced EMF for a small sample on the z axis will be, by reciprocity, proportional to $|\mathbf{B}_1(z)|$. Hence for the signal from nuclei along the axis of the coil and a depth, d, inside the conducting medium,

$$SNR \propto a^3 |\mathbf{B}_1(h + d)| \sqrt{\omega L/(r_0 + r_L(h))}. \qquad [9]$$

For finite-sized samples, an appropriate average of $\mathbf{B}_1$ over the sample volume should be used.

The analysis above can be easily extended to other configurations involving multiple co-axial loops. For example, if a second identical coil is added at a distance $(h + b)$, $b > 0$, from the conducting medium, but with the current in the opposite sense in order to form a gradiometer of "baseline b," one gets for the infinite medium

$$P_g(h) = \frac{\pi}{8} \mu_0^2 \sigma \omega^2 I^2 a^3 \left[f\left(2\,\frac{h}{a}\right) + f\left(2\,\frac{h+b}{a}\right) - 2f\left(\frac{2h+b}{a}\right) \right] \qquad [10]$$

and

$$\mathbf{B}_{1g}(z) = \frac{\mu_0}{2} a^2 I \left[\frac{1}{(a^2 + z^2)^{3/2}} - \frac{1}{(a^2 + (z+b)^2)^{3/2}} \right] \mathbf{a}_z. \qquad [11]$$

The loss integral for this case (the sum in brackets in Eq. [10], with $\beta = 2h/a$) is also shown in Fig. 1a. The *SNR* is then calculated as was done in Eq. [9]. The gradiometer loss integral drops very rapidly to zero with increasing h, and when $h = 0$, virtually all of the power is dissipated within one coil radius of the surface. The losses for the gradiometer for a finite region can be included as was done above; however, as will be shown below, corrections for a finite medium for the gradiometer are not needed in practice.

Figure 1b shows a comparison of the functional dependence of $\mathbf{B}_1(h)$ for fixed current, I, and the losses shown in Fig. 1a for smaller values of h. It can be clearly seen that near $h = 0$, the losses drop much more rapidly with increasing h than does the magnitude of $\mathbf{B}_1$ for both coils. Hence, even though the coil sensitivity is decreased with increasing h, *SNR* will initially increase with increasing h for both coils. Note also that though the maximum RF field for the circular coil is much greater than the maximum field of this short-baseline gradiometer, the losses for the circular coil at small h are also much greater than those of the gradiometer.

It is instructive to consider the semi-infinite case where the power losses in the medium dominate by setting $r_0 = 0$ above. Figure 2 shows *SNR* for the simple surface coil and gradiometer coil with $b = a/2$, both assumed to have the same inductance, L, as a function of height, h, and various sample depths, d. For samples near the surface, there is clearly a gain in *SNR* when the coil is held above the surface. Figures 3 and 4 show plots of h_{opt}, the optimum value of h for a given sample

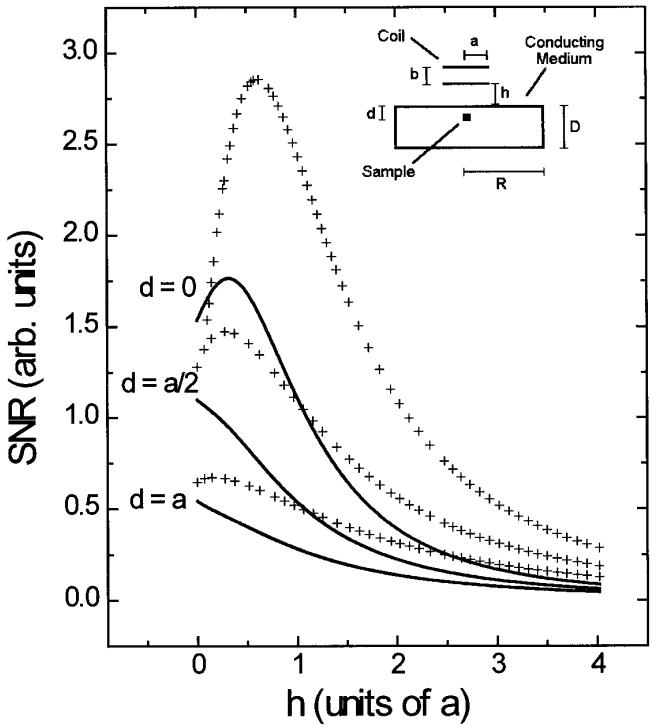

FIG. 2. Dependence of *SNR* on coil height for signals from a depth *d* for an ideal simple surface coil (solid line) and an ideal two coil gradiometer (+) with the coil spacing equal to one-half the coil radius ($b = a/2$) as computed using Eq. [9]. The inset shows the geometry used here.

depth, and the corresponding value of *SNR* for the single coil and for the gradiometer coil with various coil spacings, respectively. For the gradiometer, the single coil result is obtained in the limit of large coil spacing. Note the surprising result for this idealized case: *SNR* for the gradiometer is significantly better than that of the simple surface coil, all other factors being equal.

Calculations with $r_0 = 0$ lead to the somewhat counterintuitive conclusion that the best *SNR* will be obtained for a very closely spaced gradiometer coil ($b \ll a$) held far ($h \gg a$) from the conducting medium. Even though B_1 diminishes as the coil spacing is decreased, the losses in the medium decrease even more rapidly. However, when a nonzero value of r_0 is used to represent finite coil losses, there will be an optimum spacing and lift-off distance. In addition, one should consider the effects of the mutual inductance between the coils, which reduces L for small spacings. As will be shown below, the corrections for a finite-sized medium may also be very important for the simple circular loop coil and hence also for any comparison of the relative performance of these two coils.

Consider a gradiometer coil made from two single circular loop coils each with an inductance L and resistive loss r_0. Then the Q of the gradiometer, Q_g, away from the conducting medium (the free space Q) is given approximately by

$$Q_g = (L - M)/r_0, \qquad [12]$$

where M is the magnitude of the mutual inductance between the coils. For any specific coil, the mutual inductance falls rapidly with coil separation (*14*). For practical high-Q coils, $M \ll L$ for $b > a$, and M gives only a small correction ($\lesssim$20%) for $b \gtrsim 0.5\ a$. As b becomes less than about $0.5a$, M rises very rapidly until $M = L$ in the (unphysical) limit where $b = 0$. General expressions will require knowledge of the wire dimensions used and are not pursued here. However, an explicit comparison between a single loop coil and a gradiometer made from two single loops is easily made.

Referring to Fig. 4, we see that the optimum *SNR* for constant inductance is rather insensitive to coil spacings near $b = a/2$. However, for coils spaced closer than about $a/2$, the mutual inductance will become large, reducing Q_g, and *SNR* will be reduced. Hence, an optimum spacing will be, within factors of order unity, $a/2$.

EXPERIMENTAL

Two types of surface coils are considered here. The first is a simple circular surface coil that we may term a "magnetometer," as it responds to the net magnetic flux through the coil. The second is an axial gradiometer that essentially rejects the net flux but responds to the (linear) gradient of the flux.

Three 20-cm-diameter coils (two simple circular coils and a gradiometer) were constructed of RG401/U semirigid coax (0.64 cm o.d.) using a split-shield design (*15*, *16*). The split-shield design yields coils which are inherently electrically balanced, greatly reducing electrostatic couplings and therefore

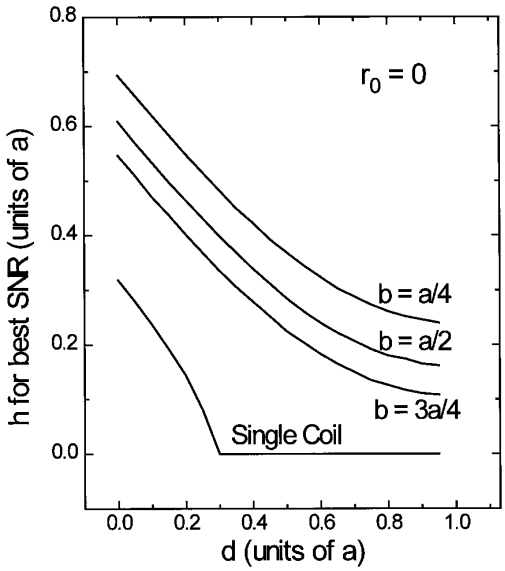

FIG. 3. The coil height, h, above the conducting medium for maximum *SNR* for the single coil and the gradiometer coil with three different coil spacings as a function of sample depth, d, in the absence of corrections for a finite-sized conducting medium and assuming the losses within the coil are negligible.

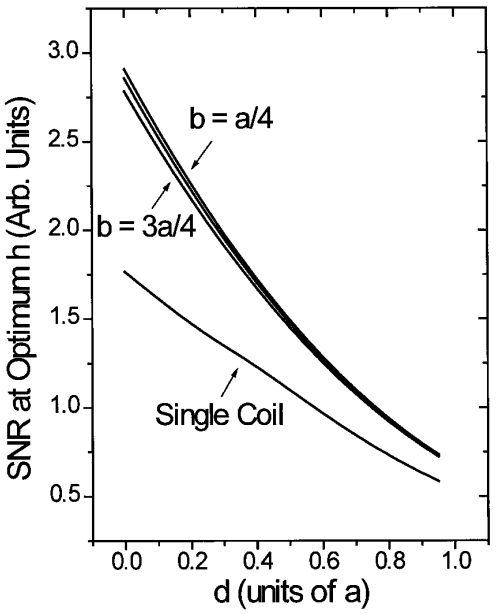

FIG. 4. The *SNR* obtained for the optimum coil heights, *h*, shown in Fig. 3. The reduction in *SNR* due to the mutual inductance between the two coils of the gradiometer has not been included here.

the loading by any nearby dielectric media. One other simple circular surface coil, 5.5 cm in diameter, was constructed in a similar manner using 0.64-cm-o.d. copper tubing. The latter was used only for measurements which did not require the central coaxial conductor.

All the coils were parallel tuned with high-Q ceramic capacitors (American Technical Ceramics[2]): see Table 1 for electrical details. The mutual inductance for the gradiometer is calculated based on Grover's tables (*14*). The inductance of the gradiometer, L_g, calculated using the inductance for the single circular coil combined with the mutual inductance is 0.648 μH, which is very close to the measured value of 0.64 μH. Values of r_0 are computed from the measured values of Q_{inf} and the inductance.

To provide an electrically lossy medium, both a 230-liter rectangular aquarium (43 $\times$ 89 cm) filled to a depth of 57 cm and a larger 6 ft $\times$ 12 ft (1.84 m $\times$ 3.69 m) pool filled to a depth of 5′ (1.53 m) were filled with artificial sea water, prepared from "Instant Ocean," to obtain measured dc electrical conductivities of $\sigma = 3.55$ S/m and, by dilution, $\sigma = 1.28$ S/m in the smaller tank and $\sigma = 0.33$ S/m in the larger tank, measured with a Hydrolab DataSonde 4. A recirculator was used to provide a uniform conductivity in the large tank. To simulate a magnetic resonance signal, a small (1-cm-diameter) untuned transmitter coil, driven by a 5-W broadband RF amplifier, was placed a fixed distance d below the surface of the water, co-axial with the surface coils.

For ^{14}N nuclear quadrupole resonance (NQR) transitions, frequencies of 0.5–5 MHz are appropriate. At 3.5 MHz, the skin depth, δ, of the conducting medium needs to be considered. Here the skin depths are 46 cm and as small as 14 cm, respectively, for the larger and smaller tanks, and so RF screening effects cannot be ignored. The RF screening was taken into account in an *ad hoc* way, by setting the depth $D = \delta$ for analysis.

The efficiencies and Q's of the coil were measured in two ways. In the first method (method 1), the surface coil was carefully matched to 50 Ω with a series capacitor, and the voltage induced by the transmitter was observed at the output of the matching capacitor. This method corresponds to the conventional observation of a magnetic resonance signal by a tuned and matched circuit, and the signal here is proportional to $B_1\ Q_m^{1/2}$, where B_1 is the magnetic field that would be induced by a unit current flowing in the surface coil, and Q_m is the quality factor under matched conditions. Most of the measurements were obtained using a second method (method 2), where a separate untuned pickup coil was mounted on the axis of the surface coil, approximately 10 cm from the surface coil (on the side of the surface coil away from the tank). The series matching capacitor from the surface coil was not terminated, and so this method measures the "unmatched Q," Q_0, of the coil. (Provided the coil is impedance-matched carefully, $Q_m = \frac{1}{2} Q_0$.) The voltage induced across the untuned, weakly coupled pickup coil is proportional to $B_1\ Q_0$: note the linear dependence on Q in this case.

A network analyzer (HP 4195A) drove the RF transmitting amplifier and monitored the voltage induced in the surface coil or the pickup coil. The values of Q were measured from the

[2] Reference to this and other commercial products is for completeness, and products from other manufacturers could also be suitable.

TABLE 1
Electrical Properties of the Coils Used for Measurements

	Diameter (cm)	Inductance (μH)	Mutual inductance (μH) (calc.)	Tuning capacitance (nF)	Q_{inf}	r_0 (mΩ)
Small circular coil	5.5	0.077	—	1.5 @ 14.8 MHz	265 ± 3	27
Circular coil 1	19.6	0.43	—	4.4 @ 3.65 MHz	380 ± 3	26
Circular coil 2	18.8	0.42	—	4.76 @ 3.56 MHz	335 ± 3	28
Gradiometer (5 cm spacing)	19.5	0.64	−0.106	3.40 @ 3.42 MHz	293 ± 3	47

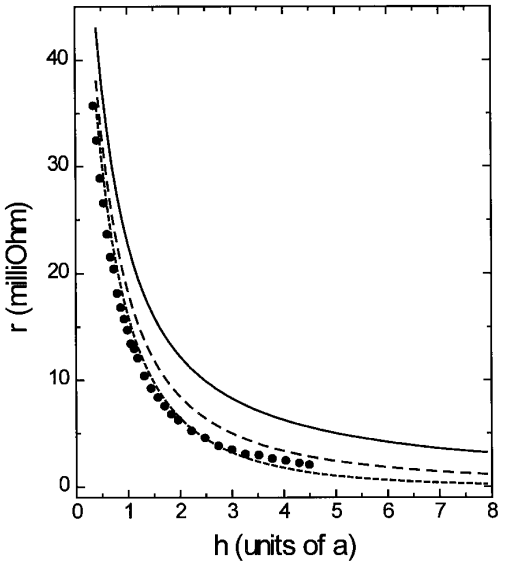

FIG. 5. The measured loss resistance, r, for the 20-cm-diameter circular coil #1 at 3.65 MHz near the large tank (circles). Theoretical predictions are shown for the semi-infinite model (solid line), the case of infinite width but finite depth (dashed line) and taking into account both the finite depth and width of the tank (dotted line). There are no adjustable parameters in this fit.

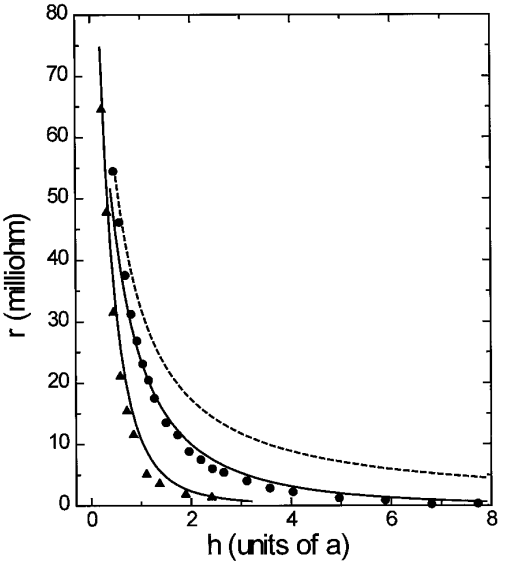

FIG. 6. The loss resistance, r, for the small circular coil at 14.8 MHz (circles) and for the 20-cm-diameter gradiometer coil at 3.4 MHz (triangles) near the small tank containing solution with conductivities of 1.28 and 3.55 S/m, respectively. The solid lines show the predictions from theory with no adjustable parameters. For the gradiometer, the semi-infinite model was used with no finite size corrections. The dotted line shows the prediction for the small circular coil without finite size corrections.

3-dB points of the response curves. Since the effective Q involves loss due to the dissipation in the medium, as well as coil resistance, loss in the capacitors, radiation loss, and dissipative loss in other more distant lossy structures in the laboratory, some care was taken to record Q_{inf}, the value of Q_0 at a substantial distance ($\geqslant$1 m) from the tank. These contributions to Q_{inf} are then subtracted from the measured Q's to isolate the dissipation ascribed to the lossy medium.

RESULTS AND DISCUSSION

Figure 5 shows the loss data for circular coil #1 of radius a = 9.8 cm (see Table 1) near the large tank, along with theoretical predictions. The tank depth and effective tank radius, R, used for the predictions were 46 cm (4.7 a) and 0.91 m (9.3 a), respectively. Even though the conducting medium is large compared to the coil radius, the corrections for the finite-sized tank are clearly necessary and, when included, yield good agreement with experimental results. Figure 6 shows similar data for the smaller circular coil and the gradiometer coil near the smaller tank along with theoretical predictions. Once again, the finite size of the tank must be included to obtain a good theoretical prediction for the circular coil; however, the semi-infinite model is quite adequate for the gradiometer coil.

For the circular coils, the finite size effects will thus be important when considering an optimum lift-off of the coil, and the values shown in Fig. 3 should not be directly used for finite conducting media. Rather, these values should be recalculated, taking into account the finite size of the particular conducting medium. This will be important for applications such as MRI, though not for landmine detection.

Figure 7 shows relative *SNR* measurements for circular coil #2 and the gradiometer coil. These were obtained, along with Q_0, with the two probe technique and each point is divided by $Q_0^{1/2}$ to correspond to the *SNR* which would be measured

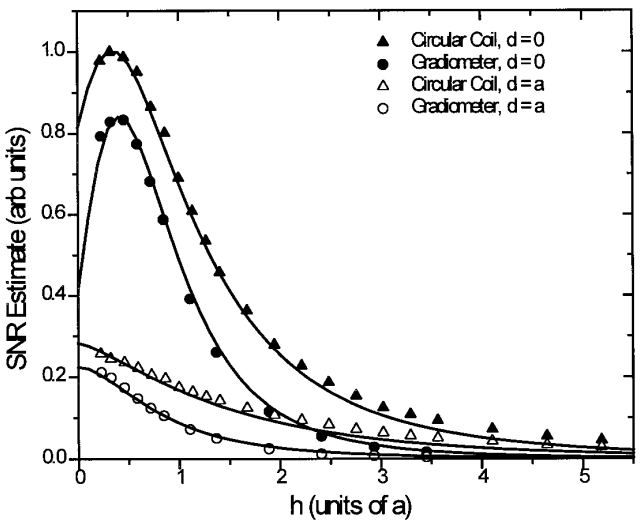

FIG. 7. Measured signal-to-noise ratio (symbols) as a function of height, h, for circular coil #2 and the gradiometer coil next to the small tank containing solution with σ = 3.55 S/m compared to theory (solid lines) which includes the finite size of the medium and losses in the coils.

under matched conditions. Since *SNR* was not measured directly, we refer to these as the estimated *SNR*. The relative scale factor between the two coils was determined using method 1 above. The only adjustable parameter in the theory here is an overall scale factor (adjusted by eye) and the agreement with measurement is quite good. For these measurements with the smaller tank, there is clearly an improvement in *SNR* for samples at the surface when a lift-off of just under $h = 0.5\ a$ is used for both coils. For deeper samples, a lift-off of $h = 0$ yields the best results.

We note that in the absence of the conducting medium and for the same input power, the circular coil generates a B_1 field more than three times greater than that of the axial gradiometer at the position (approximately $a/2$) of maximum *SNR*. In the presence of the conducting medium, the loading on the circular coil is so much greater than that on the gradiometer that the actual *SNR* is almost identical for the two coils for this case. As mentioned above, the gradiometer also has the advantage of reducing external RF interference.

CONCLUSION

A theory to calculate the extra resistive losses for a circular coil at height, h, above a conducting medium was developed and tested. Those extra losses can then be used to compute the *SNR* of magnetic resonance measurements at different coil heights above the conducting medium. It was found that for a simple circular loop, models based on an infinite conducting medium are inadequate for finite systems even with dimensions of many coil radii, though satisfactory results are obtained when finite size corrections are included. The theory was also applied to a simple gradiometer constructed with two co-axial circular loops. It was demonstrated that an infinite model is quite adequate for this gradiometer coil. It was shown theoretically that for a truly infinite medium, the gradiometer may yield a better *SNR* than does a circular loop. For finite media, which coil will yield the better *SNR* can be computed using the theory presented here. In any case, for samples near the surface of the conducting medium, *SNR* can be improved by raising the coil above the surface a fraction of a coil radius.

ACKNOWLEDGMENTS

This work is supported in part by the U.S. Federal Aviation Administration, the Office of Special Technology (U.S. Department of Defense), and the Defense Advanced Research Projects Agency. Thanks for experimental assistance go to Mr. John Pohlman, Dr. John Saylor, and Dr. Dean Stoddard of NRL.

REFERENCES

1. D. I. Hoult and P. C. Lauterbur, *J. Magn. Reson.* **34,** 425–433 (1979).
2. C. E. Hayes and L. Axel, *Med. Phys.* **12,** 604–607 (1985).
3. E. Alanen and I. V. Lindell, *Radio Sci.* **19,** 1469 (1984).
4. D. V. Trushkin, O. A. Shushakov, and A. V. Legchenko, *Geophys. Prospecting* **43,** 623–633 (1995).
5. T. Hirshfeld and S. M. Klainer, *J. Mol. Struct.* **58,** 63–77 (1980).
6. V. S. Grechishkin, *Appl. Phys. A* **55,** 505–507 (1992).
7. A. D. Hibbs, G. A. Barrall, P. V. Czipott, D. K. Lathrop, Y. K. Lee, E. E. Magnuson, R. Matthews, and S. A. Vierkotter, Land mine detection by nuclear quadrupole resonance, *in* "Detection and Remediation Technologies for Mines and Minelike Targets III," (A. C. Dubey, J. F. Harvey, and J. T. Broach, Eds.), Proceedings of SPIE, Vol. 3392, pp. 522–532 (1998).
8. T. N. Rudakov, A. V. Belyakov, and V. T. Mikhaltsevich, *Meas. Sci. Technol.* **8,** 444 (1997).
9. C.-N. Chen and D. I. Hoult, "Biomedical Magnetic Resonance Technology," pp. 160–163, Adam Hilger, IOP Publishing, New York (1989).
10. M. D. Harpen, *Med. Phys.* **14,** 616 (1987).
11. J. Wang, A. Reykowski, and J. Dickas, *IEEE Trans. Biomedical Eng.* **42,** 908 (1995).
12. P. M. Morse and H. Feshbach, "Methods of Theoretical Physics," Part II, p. 1798, McGraw–Hill, New York (1953).
13. See G. N. Watson, "A Treatise on the Theory of Bessel Functions," 2nd ed., p. 389, Cambridge Univ. Press, Cambridge, UK (1944).
14. F. W. Grover, "Inductance Calculations—Working Formulas and Tables," Dover, New York (1973).
15. (a) A. Stensgaard, *J. Magn. Reson. A* **122,** 120 (1996). (b) A. Stensgaard, *J. Magn. Reson.* **128,** 84 (1997).
16. B. H. Suits, A. N. Garroway, and J. B. Miller, *J. Magn. Reson.* **131,** 154 (1998).